

Assessment of Snowmelt Quality Discharging from a Cold-Climate Urban Landscape During Spring Melt

Hayley Popick

University of Saskatchewan

Markus Brinkmann

University of Saskatchewan

Kerry McPhedran (✉ kerry.mcphedran@usask.ca)


University of Saskatchewan <https://orcid.org/0000-0001-9718-6793>

Research Article

Keywords: Stormwater (SM), cold climate, road salts, polyaromatic hydrocarbons (PAHs), metals, *Raphidocelis subcapitata* (algae), *Vibrio fischeri* (bacteria).

Posted Date: October 26th, 2021

DOI: <https://doi.org/10.21203/rs.3.rs-952261/v1>

License:  This work is licensed under a Creative Commons Attribution 4.0 International License. [Read Full License](#)

Abstract

Stormwater results from precipitation events and melting snow running off urban landscapes and typically being released into receiving water bodies with little to no treatment. Despite evidence of its deleterious impacts, snowmelt (SM) management and treatment are limited, partly due to a lack of quality and loading data. This study examines snowmelt quality during the spring for a cold-climate, semi-arid Canadian city (Saskatoon, Saskatchewan). Four snow storage facilities receiving urban snow plowed from roads in mixed-land-use urban catchments (228 km²) were sampled including snow piles (five events) and SM (twelve events) runoff in 2019 and 2020. Samples were analyzed for pH, EC, TDS, TSS, COD, DOC, metals, chloride, PAHs, and *Raphidocelis subcapitata* and *Vibrio fischeri* toxicity. Notable event-specific TSS spikes occurred on April 13th, 2019 (3,513 mg/L) and April 24th, 2019 (3,838 mg/L), and TDS, chloride, and manganese on March 26th, 2020 (15,000 mg/L, 5,800 mg/L, 574 mg/L), April 17th, 2020 (5,200 mg/L, 2,600 mg/L, 882 mg/L), and April 23rd, 2020 (5,110 mg/L, 2,900 mg/L, 919 mg/L), though chloride remained elevated through May 1st, 2020 samples (1,000 mg/L). Additionally, at two sites sampled April 13th, 2019 pulses of aluminum (401 mg/L) and PAHs (pyrene, phenanthrene, anthracene; 71 µg/L, 317 µg/L, 182 µg/L) were detected. The EC₅₀ for *R. subcapitata* and *V. fischeri* was observed, if at all, above expected toxicity thresholds.

1.0 Introduction

Stormwater (SW) is water resulting from precipitation events and melting snow, running off the urban landscape, collecting in storm sewers, and being released into the environment with little to no treatment. Increasing urbanization in cities has sealed soils, removed vegetation, and changed natural drainage paths resulting in increased quantities and flashiness of SW discharging from these landscapes, in conjunction with significantly decreased SW quality (Yang and Toor 2017; Zgheib et al. 2008). Untreated SW is recognized as a significant transport vector for contaminants to enter receiving water bodies (Barbosa et al. 2012; Blecken et al. 2012; Matos et al. 2015; Qinqin et al. 2015). In cold climates, precipitation falls as snow during the winter, introducing an additional form of runoff that depends on snow management practices. Interest in urban snowmelt (SM) quality started in the late 20th century in places such as Europe and Canada (Schrimpff et al. 1979; Zinger and Delisle 1988), with increasing research since the 1990s (Mayer et al. 1999; Oberts et al. 2000; Viklander 1996, 1999; White et al. 1995). Interestingly, studies typically examine road runoff (Helmreich et al. 2010; Legret and Pagotto 1999; Taka et al. 2017; Westerlund and Viklander 2006) as opposed to runoff from snow storage facilities which can potentially contain snowpack-derived transformation chemicals (Exall et al. 2011a; Shotyk et al. 2010).

The impact of SW depends on the concentration and mixture of contaminants, which are themselves influenced by climatic and land-use conditions within the catchment (Aryal et al. 2010; Matos et al. 2015). In cold climates, urban snow is often managed by pushing snow to the sides of the road, application of road salt and/or sand, and collection of snow for delivery to snow storage sites. Prior to collection and within hours of traffic exposure (Glen and Sansalone 2002) the snow accumulates contaminants such as total suspended solids (TSS) (Sillanpää and Koivusalo 2013), metals (Kuoppamäki et al. 2014), organics (Hemgren et al. 2010; Howitt et al. 2014), and total dissolved solids (TDS), notably chloride (Reinosdotter and Viklander 2007; Westerlund and Viklander 2008). Whether they bank the road or occupy storage sites, snowpacks (noted as SP herein) are highly-permeable media susceptible to heat and mass fluxes (Albert and Hardy 1995; Calonne et al. 2012; Ebner et al. 2016; Löwe et al. 2011). The unique physicochemical traits of snow as a SW matrix can influence the concentrations of contaminants within the pack (Ebner et al. 2016) and create chemical transformation products (Glen and Sansalone 2002).

The form in which contaminants are found is known to effect potential toxic impacts by affecting bioavailability to aquatic organisms; in SM, elevated concentrations of Cd, Cu, Mn, Ni, and Zn have been associated with elevated chloride ion concentrations (Lazur et al. 2020; Mayer et al. 2011a; Reinosdotter and Viklander 2007). The chloride ion from road salts drives toxicity in *Lampsilis* freshwater mussels (Prosser et al. 2017) while road salts and dissolved Zn were most closely associated with toxicity endpoints in *Ceriodaphnia dubia* and *Oncorhynchus mykiss* (Mayer et al. 2011a). Most heavy metal burdens in urban SM (>90%) were in the particulate phase which remained on the snow storage site (Westerlund and Viklander 2011). Despite potentially reducing the acute aquatic toxicity of SM runoff, these contaminants may instead be transferred to adjacent benthic ecosystems (Karlavičiene et al. 2009; Rentz et al. 2011) or into subsurface and groundwater flows (Mohammed et al. 2019; Pavlovskii et al. 2019; Shotyk et al. 2010).

In SW models, contamination is considered to be deposited on the urban landscape in a linear or asymptotic fashion between storm events with some/all contaminants being carried into the SW during the preceding rainfall event (Barbosa et al., 2012; LeBoutillier et al., 2000). Mobile substances such as salts are washed first, while heavier or particle-bound contaminants may require high volumes or intensities to flow into sewers (Mayer et al. 2011b). This phenomenon is referred to as the 'first flush', and though it is used in SW to

refer to a single-event phenomenon, the mechanisms of pollutant build-up and wash-off also influence spring melt runoff characteristics. As snow melting occurs on warm days contaminants are preferentially eluted from the SP (Westerlund et al. 2008; Westerlund and Viklander 2006) causing an SM-driven discharge to receiving water bodies. This occurs in both SPs at storage facilities and those undisturbed within the catchment, with the latter uptaking contaminants as governed by land-use classes before entering the sewer similarly to summer SW.

While urban SW quality is well-researched, it is often conducted in climates that receive limited or no snowfall (Galfi et al. 2017; Westerlund and Viklander 2011). Spring SM in cold regions may contribute up to 60% of the annual contaminant loading into receiving environments (Oberts et al. 2000). Despite the potential impacts of this loading the literature body of urban SM quality, transport, and modeling remains limited (Bartlett et al. 2012; Codling et al. 2020; Galfi et al. 2017; Mayer et al. 2011a; Moghadas et al. 2016; Sillanpää and Koivusalo 2015; Taka et al. 2016; Valeo and Ho 2004; Valtanen et al. 2014; Vijayan et al. 2019; Westerlund and Viklander 2011). Though the toxic potential of winter road runoff to vertebrates is well-discussed (Hintz and Relyea 2017; Hopkins et al. 2013; Meland et al. 2010; Sanzo and Hecnar 2006), few studies examine runoff discharging from urban facilities (Exall et al. 2011) or conduct invertebrate bioassays (Mayer et al. 2011a; Prosser et al. 2017). The spring runoff at these facilities is subject to longer holding conditions than road runoff which is removed expediently. Furthermore, spring runoff draining to SW sewers will follow the same transport path as summer SW and uptake similar characteristics from the landscape. This could confound differences between spring SM and summer SW necessary to determining the impact of SM on its immediately adjacent environments. Previous observations indicate plowed snow is significantly more burdened than undisturbed SPs, containing up to 50% of areal pollutant mass (Kuoppamäki et al. 2014; Moghadas et al. 2015; Sillanpää and Koivusalo 2013; Viklander 1999). Thus, the goal of this study was to assess the quality of urban snow collected and stored in municipal snow storage facilities in the City of Saskatoon (CoS), Saskatchewan, Canada. The CoS is in a cold-climate, semi-arid region of Canada and borders both banks of the South Saskatchewan River (SSR) which is the receiving waterbody for city SW. Previous research into the CoS's SW runoff quality has been conducted (Al Masum et al. 2021; Codling et al. 2020; McLeod et al. 2006; Challis et al., 2021; Popick et al. 2021), however, no previous study has considered SM runoff quality. The SM quality assessment includes analysis of pH, electrical conductivity (EC), total dissolved solids (TDS), total suspended solids (TSS), chemical oxygen demand (COD), total organic carbon (TOC), dissolved organic carbon (DOC), dissolved metals, chloride, and targeted dissolved polyaromatic hydrocarbons (PAHs). In addition, SM toxicity was assessed using *Raphidocelis subcapitata* and *Vibrio fischeri*. Lastly, land use classifications are used to determine potential pollutant loadings into the SSR following similar assessments for rainfall-only SW presented by Al Masum et al. (2021) and Popick et al. (2021).

2.0 Methods

2.1 Study Area

The CoS has a total area of 228 km² and a population of about 330,000 making it the largest municipality in Saskatchewan (Statistics Canada 2021). Based on climate data collected by the Saskatchewan Research Council's Climate Reference Station (CRS), the average daily temperature ranges between approximately 18.7°C in August and -14.7°C in January, with an annual average of 3°C. The CoS receives an average of 355 mm of precipitation per year, with ~50 mm of precipitation falling between the months of November and March as snow.

There are four snow storage facilities within the CoS, all of which were included in the present study (Figure S1). These sampling sites include the impermeable site on the southwest border of the CoS (**Valley Rd.**), one site north of the CoS along **Wanuskewin Rd.**, one site located in the northeast of the city (**Central Ave.**), and one located within the University of Saskatchewan grounds (**USask**). The Valley Rd. site has a paved surface, a settling pond, and a designated outlet where the meltwater enters a series of specially designed barriers before being discharged into the SSR. The other three sites do not regulate SM flow and lie adjacent to vegetated wetlands or swales. Storage facility sites are noted with a blue dot, while red dots note SW outfalls which were sampled as part of a parallel study. See Supporting Information (SI) for snowfall information used in the current studied expressed as snow-water equivalents (SWE) (Table S1).

2.2 Sampling

Snow was collected from at least one of the four snow facilities on warm days in which SM was being created (Table S2). Snow directly from the pile (SP) sampled four times in April 2019, and SM puddles were sampled eleven times from March to May 2020. One SM sample was obtained on April 2nd, 2019 and two SP samples were obtained on March 7th, 2020 for SP-SM comparisons within site and event. Plastic scoops were used to collect both snow and SM in pre-cleaned 4-L or 25-L Nalgene containers. Snow from the piles was collected from 8-12 random locations on the surfaces and sides of the SPs to create an aggregate sample. The SM samples were

obtained from meltwater pools found at the foot of SPs and also collected from 8-12 locations from on-site puddles to create an aggregate sample of the SM. Samples were sealed, labelled, and transported to the USask Environmental Engineering labs for storage at 4°C. SP samples were melted in their Nalgene containers at 21°C in the labs for initial analyses before storage at 4°C.

2.3 Laboratory Analyses

Laboratory-based analysis included physicochemical, biological, and toxicity assessments. Physicochemical analyses of samples included pH, TSS, TDS, EC, COD, TOC/DOC, metals, PAHs, and chloride. The SP density (kg/m^3) was calculated by packing snow from the April 2nd, 2019, and April 13th, 2019, snow events into a plastic container, estimating the volume, weighing, melting the snow at room temperature, measuring the volume, and then using the difference in volume to calculate density. The biological analyses comprised the enumeration of fecal coliforms, while twotoxicity assays were conducted including *Raphidocelis subcapitata* algae and *Vibrio fischeri* bacteria.

2.3.1 Physicochemical Analyses

The TSS concentration was measured *via* vacuum filtration using Whatman™ 934-AH™ glass microfibre filters following Standard Methods 2540 (2018). A HACH sensION 156 digital probe was used to measure pH, TDS, and EC. For DOC, all samples were extracted through a 0.45- μm Teflon filter using a 12-mL Luer-Lock syringe. Approximately 40 mL of filtered sample was placed in a glass vial and analyzed using a Lotix combustion TOC analyzer (Teledyne Tekmer, OH, USA) following the manufacturer-provided method. For COD, samples were added to VWR Mercury-Free High-Range (20-1,500 mg/L) COD digestion vials and the COD was measured using a HACH DR/4000U Spectrophotometer (HACH USA, CO, USA) set to 625 nm following the HACH COD Method 8000 (HACH 2014). Samples were run in duplicate using either 2 mL of sample or 1 mL of sample and 1 mL of distilled (DI) water. Chloride concentrations were determined by Bureau Veritas (Calgary, Canada) using Auto Colourimetry.

For metals analysis, samples were acidified with 0.02 N nitric acid and vacuum-filtered through a 0.45- μm nitrocellulose filter. A 100-mL sample volume was passed through the filter and the filtrate was collected in a Nalgene container. Samples were analyzed using Inductively Coupled Plasma Mass Spectrometry (ICP-MS) at the USask Department of Geological Sciences or the USask Toxicology Centre. The methods at the Department of Geological Sciences included the use of a PerkinElmer 300D ICP-MS, diluting samples 20x prior to analysis, and using a custom calibration standard (SCP Science) for blanks and standards of 10, 50, and 100 ppb. The certified reference material was NIST-SRM1643f. At the Toxicology Centre, samples were analyzed using an Agilent 8800 ICP-MS QQQ Triple Quadrupole mass spectrometer (Agilent, Santa Clara, USA). OminiTrace Ultra nitric acid (HNO_3) (w/w) (Millipore-Sigma, Ontario, Canada) was used for blanks, standards, and sample solutions. High-purity standard stock solutions (1000 mg/L) were purchased from Delta Scientific (Mississauga, Canada). The calibration standard solution, containing 22 multi-elements, was supplied by SCP Science (Quebec, Canada). The standard reference material, natural water 1640a, was supplied by National Institute of Standards and Technology (NIST) (Gaithersburg, USA).

Samples for PAH analyses were pre-filtered (Whatman™ 934-AH™ glass microfibre filters) to remove high TSS concentrations prior to solid-phase extraction (SPE) to eliminate clogging of the filter. After filtration, 2 mL of chloroform was added per 1 L of sample as a preservative, with the samples stored in amber glass bottles at 4°C prior to extraction. A deuterium-labelled internal standard mix (500 mg/L of acenaphthene- d_{10} , chrysene- d_{12} , and phenanthrene- d_{10} in acetone) provided by Sigma Aldrich (Oakville, ON) was added to the sample at a 10 $\mu\text{L/L}$ ratio. Before sample addition, Waters Oasis HLB 500 mg extraction columns were pre-conditioned using 3 mL dimethylene chloride (DCM), 3 mL methanol (LC-MS grade), and 3 mL 18.2 M Ω -cm ultrapure water (EMD Milli-Pore Synergy® system, Etobicoke, ON). Up to 500 mL of each SM sample was vacuum extracted through the column at a rate of 1 drop/second. After extraction, the column was washed with 3 mL of 5% methanol in water and air-dried with suction for 10-30 minutes. If column elution was not possible immediately following extraction, the columns were stored at -20°C. Columns were eluted twice with 5 mL of DCM and once with 5 mL of methanol. The eluate was collected in glass vials, reduced to a volume of 10 mL with a gentle stream of nitrogen gas, and split into two 5-mL portions (one portion used for a parallel research study). The aliquots were reduced to near dryness under nitrogen and reconstituted in 0.5 mL nonane. The reconstituted sample was added to a gas chromatography vial and stored at 4°C.

Samples were analyzed for PAHs using gas chromatography-mass spectrometry (GC-MS) using A Thermo Scientific Trace 1300 or 1310 gas chromatograph coupled with a Thermo ISQ 7000 single quadrupole or a Thermo QExactive quadrupole-Orbitrap hybrid mass spectrometer, respectively. Helium (99.999% purity) was used as the carrier gas to separate the PAHs on an Agilent DB-5ms (60 m x 250 μm I.D., film thickness 0.1 μm) fused silica capillary column. Both instruments were operated in full scan mode, and data were analyzed using an isotope-dilution workflow, i.e., areas of target compounds were normalized to the areas of recovered deuterium-labelled

standards. A seven-point calibration curve, along with extraction and solvent blanks were run with each batch of samples. Limits of detection and quantification are included in Table S3.

2.4 Biological and Toxicity Analyses

The first toxicity assessment was the inhibition of the luminescence of *V. fischeri* aquatic bacteria. The method is described in EPS RM/1/24 (Environment Canada 1993) using a Microtox M500 machine (Modern Water, DE, USA). Phenol (60 mg/L) was used as the positive control and 20% sucrose as both the diluent (SD) and Osmotic Adjustment Solution (OAS) as recommended for freshwater samples or increased test sensitivity to metals. The SD was also used as the negative control. This method was adapted to measure the luminescence inhibition of dilution series in 96-well microplates using an OptimaSTAR plate analyzer. Prior to the test, 10 mL each of the samples, OAS, and SD were refrigerated for one hour before being transferred to 25-mL beakers. Plates were run both inoculated and uninoculated to correct for background luminescence. To inoculate the wells, 1 mL of Microtox Reconstitution Solution was mixed with a vial of lyophilized *V. fischeri* strain NRRL B-11177 (Modern Water, USA); 0.3 mL of this solution was further diluted with 3 mL of SD. This solution was placed in a multichannel pipette reservoir on ice. Placing the plates on a paper towel over ice and using a multi-pipettor, plates were inoculated with 8 μ L of the bacteria solution. Luminescence readings were taken immediately, after 5 minutes, and after 15 minutes, with plates remaining on ice between measurements. Due to the configuration of the plate, samples were run as seven-step dilutions while the phenol was a six-step dilution series. Values for both samples and phenol are reported as the EC₅₀ and EC₁₀ relative to the negative control at 15 minutes.

The second bioassay tested the 72-hr chronic toxicity of *R. subcapitata* green algae following the EPA Method 1003.0 (EPA 2002). Prior to analysis, a dilution series of inoculated algae stock was used to establish a linear relationship between chlorophyll expression and cell count. The chlorophyll in *R. subcapitata* was found to relate linearly with cell count ($R^2 = 0.9996$) and this was used as a parameter for growth inhibition in that species. Samples were prepared in 1-mL wells of 24-well microplates in a configuration of four replicates of negative control and a five-step dilution series. Wells were inoculated with 100 μ L of inoculum (1,000,000 cells/mL) to meet appropriate cell densities (10,000 cells/mL in wells at the start of the test). Using fluorescence as a proxy for algae cell count, growth inhibition was measured as a function of fluorescence at 0 h and at 72 h. Cell counts were observed directly from one random control well per plate at 0 h to ensure proper inoculation. Both algae fluorescence and cell counts were read using the Tecan Spark® multifunction plate reader (Tecan Trading AG, Switzerland). Sample concentration in wells ranged from 100–6.25%, both inoculated and uninoculated to account for background fluorescence. Initially, the EC₅₀ at 72 hours was calculated; as the EC₅₀ was not observed at the full concentration for all samples, the EC₁₀ was additionally calculated (see Statistical Analysis section).

2.4.1 Land use analysis

The volume of snow transported to municipal storage facilities can be estimated using the volume of snow that is plowed from local traffic surfaces. These snowbanks are removed and hauled to municipal snow storage facilities where they are piled outdoors until they melt during spring and/or summer. The volume of snow plowed to the side of the road is assumed to be equivalent to the volume ultimately transported to snow storage sites, thus providing a quantitative estimate of snow volumes managed at the CoS's snow storage sites. However, it should be noted this volume could be partly lost to sublimation or melting over the winter, and an assessment of SP volume immediately prior to melt will most accurately reflect the impact of that melt period. Moreover, facility snow likely contains approximately half of all winter contaminant mass loads (Sillanpää and Koivusalo 2013). Though this snow may not be indicative of non-traffic related land use impacts, it nonetheless represents a significant portion of potential urban stormwater loading into receiving environments. Land-use breakdowns for the CoS are included in Table S4 which include each of the local subcatchment characteristics.

As SM discharges from the storage facilities are not currently measured in the CoS, event-mean-concentrations (and corresponding site-mean-concentrations) could not be calculated as more typical for rainfall-based stormwater events (e.g., Popick et al., 2021). Seasonal loading can be estimated, however, using the seasonal mean concentrations measured at each site in relation to the volume of estimated SM discharging from that facility. The runoff volume, in snow-water-equivalents (SWEs), was calculated using SP volume estimation and lab-measured values of late-winter SP density. Currently, Valley Rd. was selected for UAS-LIDAR imaging as it is the main snow facility in the CoS and receives approximately half of the CoS's plowed snow. UAS-LIDAR imaging of the snow facility was completed to determine the Valley Rd. site snow volume (50% of the CoS) and the remaining volumes were estimated at 25% each for the Wanuskewin Rd. and Central Ave. facilities (Table 3). The USask storage facility is markedly smaller than these other city-wide facilities, thus, the volume of snow was estimated based on GIS-based maps in comparison to the Valley Rd. site. Using the SWEs and

site-specific physicochemical and contaminant concentrations, seasonal loadings were estimated for the 2020 SM season (Table 3) as presented in the Results and Discussion.

Table 3

Snowmelt loading estimates for 2020 coming from each of four storage facilities included in this study. Note that the snowmelt volumes are based on snow-water-equivalents (SWEs) that were determined using estimates of snow volumes on site and the snowpack density (see Methods for further information).

Site	Snowmelt Volume (m ³)	Estimated 2020 Seasonal Loading (kg)											
		TDS	TSS	COD	DOC	Cu	Cr	Mn	Ni	Pb	Se	Zn	ΣPAHs
Valley Rd.	79,000	169,231	37,045	24,524	611	1.18	0.29	23.5	0.88	0.09	0.08	7.92	0.03
USask	10,000	4,624	12,563	2,781	44	0.34	0.01	0.83	0.07	0.01	0.02	0.67	0.01
Wanuskewin Rd.	34,500	5,123	32,611	8,614	53	0.36	0.07	0.40	0.18	0.02	0.01	1.03	0.01
Central Ave.	34,500	46,723	36,981	12,230	199	0.37	0.08	0.47	0.25	0.02	0.02	1.98	0.02
TOTAL	158,000	225,701	119,200	48,149	907	2.25	0.45	25	1.38	0.14	0.13	12	0.07

2.4.2 Statistical Analysis

Statistical analyses were run using GraphPad Prism 9 (GraphPad Software, San Diego, CA). Gaussian distribution of SP and SM datasets were assumed, though these sets were analyzed separately and later compared. Ordinary One-Way Analysis of Variance (ANOVA) was run to examine any site- or event-related variance in runoff characteristics ($p \leq 0.05$) along with Tukey's post-hoc test such that all samples would be intercompared. Pearson's correlations (with two-tailed P value analysis to determine if correlation was due to random sampling) were run to examine any potential relations between pH, TDS, chloride, and EC; chloride and dissolved metals; and the EC₁₀ values of *R. subcapitata* and *V. fischeri* against individual SW parameters and metals and PAH species.

To prepare the algae and Microtox data for statistical analysis, the background chlorophyll or luminescence of uninoculated samples was subtracted from that of inoculated samples to remove any baseline. The exponential growth rate between the initial and endpoints was calculated for the algal bioassay. Both algal growth rates and bacterial luminescence values, respectively, were normalized as a percent of the average chlorophyll (*R. subcapitata*) or luminescence expression (*V. fischeri*) observed in the negative control. Within GraphPad Prism, four-parameter logistic regression was used to fit dose-response curves to the growth rate and luminescence inhibition data, respectively, to obtain the EC₅₀ and its 95% confidence interval (CI) for each analyzed sample. As the EC₅₀ was not observed for many samples, the EC₁₀ and its 95% CI was also interpolated from the curve. The EC_x is defined as the concentration of the bulk SW sample required to reach the endpoint.

3.0 Results And Discussion

The Results and Discussion will be considered in three sections including: (1) Physicochemical parameters; (2) Toxicity assessments; and (3) Land-use management. The physicochemical analyses section will include a discussion of results in three subsections covering the pH, TDS, and EC (Section 3.1.1); DOC, COD, and TSS (Section 3.1.2); and metals and PAHs (Section 3.1.3). The toxicity section presents the two toxicity assays *R. subcapitata* (Section 3.2.1) and *V. fischeri* (Section 3.2.2). The final land-use section will be used to discuss the impacts of land-use on the individual catchment area estimated pollutant loadings into the SSR. Figure 1 presents a map of the CoS and a summary of all physicochemical, metals, and PAH data in the form of box and whisker plots. Further details will be discussed in each of the following subsections. Results by event are included in Table 1 (see Table S5 for results by site; Tables S6-S7 for full SP and SM results).

Table 1

Physicochemical parameters for 2019 snow pile (SP) and 2020 snowmelt (SM). Values are average (standard deviation) for all sites sampled on each occasion. Yearly values are shown in **bold**. Averages of individual events.

Date	Sites	pH	TDS	EC	DOC	COD	TSS
			(mg/L)	(μ S/cm)	(ppm)	(mg/L)	(mg/L)
Apr 2, 2019	1	8.21(0.78)	156(186)	321(381)	3.68(2.45)	202(62.6)	540(47.4)
Apr 13, 2019	3	9.10(0.18)	30.5(3.1)	64.1(6.8)	2.94(1.75)	684(7.4)	2,736(706)
Apr 18, 2019	3	9.41(0.02)	25.6(1.5)	54.7(3.1)	1.11(0.25)	324(108)	1,432(456)
Apr 24, 2019	4	9.27(0.08)	25.8(4.6)	55.0(9.5)	2.35(2.36)	438(122)	1,668(1,450)
Average (SD)		9.00(0.54)	59.4(64.1)	124(131)	2.52(1.09)	412(205)	1,594(903)
Mar 7, 2020	2	7.77(0.24)	1,446(1,098)	2,812(2,044)	12.0(5.67)	241(43.8)	1,253(940)
Mar 26, 2020	1	7.75	8650	15,370	27.4	646	40.5
Mar 29, 2020	1	8.41	1331	2,620	6.13	231	312
Apr 10, 2020	1	8.63	1200	2,370	3.83	138	225
Apr 17, 2020	6	7.53(0.36)	1,677(1,967)	3,178(3,597)	9.00(4.68)	295(157)	503(678)
April 20, 2020	1	8.00	981	1,949	6.04	193	131
Apr 23, 2020	4	8.04(0.27)	2,126(2,263)	3,989(4,127)	4.18(4.24)	242(154)	242(124)
Apr 28, 2020	3	8.16(0.39)	1,434(415)	2,803(787)	2.30(3.17)	210(107)	1,210(1,537)
May 1, 2020	1	7.94	1,721	3,350	7.62	199	244
May 5, 2020	3	8.19(0.09)	532(346)	1,073(691)	6.22(3.12)	124(66.4)	247(114)
May 12, 2020	3	8.17(0.08)	417(311)	845(617)	1.13(0.77)	121(26.4)	225(121)
Average (SD)		8.07(0.31)	1,900(2,290)	3,561(4,017)	7.80(7.17)	237(146)	421(416)

Previous studies have collected snow by sampling SPs at different depths (Calonne et al. 2011; McLaren 1982), by coring, or by simple grab sampling of the top 20 cm of the SP (McLaren 1982) and SM runoff by scooping samples from puddles (Kuchta and Cessna 2009). However, studies sampling SPs are limited and there is no standard procedure for sample collection available. Due to the mixing of various roadside snows in removal trucks, their deposition on top of old packs, and potential-freeze thaw events causing partial or preferential elution of contaminants, it was assumed pollutants would not be uniformly distributed in the pile. Previous research on pollutant loading in snow packs found grid sampling to best minimize variations in mass load estimates (Vijayan et al. 2021), though this team used drills to minimize depth uncertainty, which was not performed in the current study.

3.1 Physicochemical Parameters

3.1.1 pH, Total Dissolved Solids (TDS), and Electrical Conductivity (EC)

The average pH for SP samples was 9.00 ± 0.54 and 8.07 ± 0.31 for SM samples (Table 1). No variation was observed across either SP or SM by site or event for pH with one exception ($p \leq 0.05$): the March 7th, 2020 SP samples were significantly different from all 2019 samples. Generally, pH was significantly higher in SP samples than in SM samples ($p \leq 0.05$). Curiously, USask SP samples possessed the lowest pH of all SP samples on April 2nd, 2019 (pH = 8.76) and March 7th, 2020 (pH = 7.56) (Table S6), with pH increasing over the 2019 season (which was not observed at other sites). Due to the low SP sampling size, more field seasons are needed to confirm if lower pH and melt trends are characteristic to the site. Compared to other sites sampled on the same dates, Central Ave. SM typically had lower pH values, while Wanuskewin Rd. SM had higher pH values (Table S7). For SP samples, pH had strong inverse correlation with TDS ($R = -0.938$) and EC ($R = -0.937$), though this was driven by TDS content in March 7th, 2020 SP samples. This correlation was not observed in SM samples with $R = -0.243$ and $R = -0.247$, respectively).

The EC and TDS are related parameters so will be discussed together herein. The average EC for SP and SM were 124 ± 131 μ S/cm and $3,561 \pm 4,017$ μ S/cm, respectively, while the average TDS were 59.4 ± 64.1 mg/L and $1,900 \pm 2,290$ mg/L respectively (Table 1). No site

variation was observed for EC nor TDS for SP or SM ($p \leq 0.05$). Event-wise, with respect to SP and similarly to pH, the March 7th, 2020, samples differed significantly from 2019 samples for both TDS and EC ($p \leq 0.05$). With respect to SM, variation was observed between March 26th, 2020 and April 2nd, 2019 (TDS only), April 17th, 2020, April 23rd, 2020 (TDS only), and all samples after April 28th, 2020 (inclusive) ($p \leq 0.05$). No significant differences were observed between any other events. Except the March 7th, 2020 SP Valley Rd. and USask samples, EC and TDS results for SP samples were 1-2 orders of magnitude lower than those of SM samples. Most SM samples display elevated EC and TDS relative to summer SW, with the March 26th, 2020, Valley Rd. sample having a TDS 7-fold and an EC 6-fold greater than those of 2019 SW (collected as part of a parallel study). Though no seasonal trends were observed during the 2019 season due to elution of TDS from the SPs, the TDS in 2020 SM samples remained elevated throughout the sampling season (Table 1), driven by individual site-specific contaminant spikes (Table S7), with a pulse of 1,721 mg/L TDS and 3,350 $\mu\text{S}/\text{cm}$ observed at Valley Rd. as late as May 1st, 2020.

Measurements of chloride were performed on select samples (Table S8). Generally, chloride comprised 39-67% of TDS concentrations, except the April 28th, 2020, USask sample, where it only comprised 11% of TDS (the value returned to a set-typical value on May 5th). Compared to summer SW chloride concentrations (141 ± 56 mg/L), concentrations on April 2nd, 2019 SM were similar (150 mg/L) but chloride was more abundant in less-melted March 7th, 2020 samples. Mirroring TDS and EC concentrations, USask SP contained more slightly more chloride than SM, while at Valley Rd. significantly more chloride was observed in SM. Making this observation within chloride as opposed to TDS is interesting: 62% of the TDS burden in the Valley Rd. SM sample is chloride (46% in SP), while this proportion is only 41% in USask SM (47% in SP). The sites are evidently within different stages of preferential elution early into the sampling season, likely due to the unique impervious surface at the Valley Rd. site. Throughout the 2020 spring melt the largest three pulses of chloride are observed at this site (2,600-5,800 mg/L), with the next largest three pulses observed at Central Ave (1,100-1,700 mg/L). As chloride encourages dissolved partitioning of metals, correlations between chloride and metals concentrations were examined. There is some correlation between the presence of chloride and dissolved concentrations of arsenic ($R = 0.594$), cadmium ($R = 0.489$), manganese ($R = 0.684$), nickel ($R = 0.658$), and strontium ($R = 0.482$) in tested samples, the implications of which are further discussed in Section 3.2.

A two-week melt period was observed prior to sampling in April 2019, which was not observed in March 2020. Additionally, the seasonal sampling events on April 2nd, 2019, and March 7th, 2020, took place on cooler days relative to other events. Both sampling conditions may explain the relative similarity in pH (as temperature governs the chemical composition of the SW matrix), but differences in EC and TDS. As dissolved contaminants in snow are preferentially eluted with meltwater out of SPs (Viklander 1996), it is expected that EC and TDS would be elevated in SM relative to SPs. In cold climates, these parameters are a major concern for toxic impact due to the practice of road salting (Exall et al. 2011b; Mayer et al. 2011a; Murphy et al. 2014). Dissolved salts, especially chloride, affect the partitioning of metals, increasing those in the dissolved phase (Bäckström et al. 2004; Galfi et al. 2017; Mayer et al. 2011b; Reinosdotter and Viklander 2007). A previous study conducted over a period of 2 years found significantly elevated EC, TSS, TOC, copper, and zinc in melt season samples compared to rain-season samples (Helmreich et al. 2010). However, the chemodynamics of snow are complex. For example, when sand is used as an anti-slip agent (often in combination with NaCl or MgCl_2 , CaCl_2 salt), SM pH and TSS are elevated. This may counteract the dissolving effect of chloride by providing more particulate surfaces for contaminants to bind (e.g., metals, PAHs). Some of the highest SM pH values in this study occurred in Valley Rd. samples, the impermeable surface of which would retain TDS and TSS in SM runoff.

3.1.2 Dissolved Organic Carbon (DOC), Chemical Oxygen Demand (COD), and Total Suspended Solids (TSS)

Despite the presence of geese contributing organic waste onsite throughout the melt season (personal observation of H.P.) at the USask and Central Ave. sites, no site-wise significant variation in DOC nor COD was observed for either SP or SM ($p \leq 0.05$). The average DOC of SM (6.93 ± 6.25 mg/L) approximately double than that of SP (3.12 ± 2.73 mg/L). Average COD did not follow a similar trend, with SP COD (460 mg/L) slightly higher than SM COD (353 mg/L). There was significant variation in COD obtained from both pile ($\text{SD} \pm 230$ mg/L) and melt ($\text{SD} \pm 293$ mg/L) samples. Unsurprisingly, there was little correlation between COD and DOC concentrations in SP ($R = -0.068$); conversely, COD and DOC were correlated in SM ($R = 0.668$). The highest DOC values in SP occurred in USask samples (4.45 ± 1.75 mg/L; Table S5) for all 2019 events. In SM, the highest DOC values occurred in Valley Rd. samples on March 7th, 2020 (20.4 mg/L) and March 26th, 2020 (27.4 mg/L). The highest COD values were measured in April 13th, 2019, pile samples (684 ± 7.4 mg/L) and March 26th, 2020, Valley Rd. sample (645 mg/L ± 301 mg/L). For SP, event-wise differences in DOC were observed between March 7th, 2020 and April 13th, 18th, and 24th 2019 ($p \leq 0.05$); the sole differences in event-wise COD were observed between April 13th, 2019 and all other SP samples ($p \leq 0.05$). For SM, one event-specific variation in DOC occurred between March 7th, 2020 and May 12th, 2020 (p

≤ 0.05); only the March 26th, 2020 event otherwise differed from April 2nd, 2019, April 10th, April 17th, April 23rd, April 28th, May 5th, and May 12th, 2020 samples ($p \leq 0.05$). Only the March 26th, 2020 and May 12th, 2020 samples had significantly different COD from one another. The concentrations of both DOC and COD fluctuated between sites and sampling events for both SP and SM with no clear seasonal trend, though no COD values exceeding 300 mg/L were measured in SM samples after April 23rd, 2020.

The overall range of TSS varied from 31 to 2,982 mg/L in SM and 506 to 3,513 mg/L in SP. Generally, SP samples contained more TSS than SM samples, with an average TSS ($1,662 \pm 750$ mg/L) four times that of SM (400 ± 387 mg/L) (Table 1). It is not unexpected that coarse TSS remain within the SP as opposed to becoming entrained in SM runoff (Westerlund and Viklander 2011). No significant difference related to site nor event was observed for any samples. The highest TSS was observed on April 13th, 2019 SP. Elevated TSS values in SM were observed on April 17th, 2020 (USask, 1,800 mg/L), and April 28th, 2020 (Central Ave, 2,982 mg/L), coinciding with warm days in which higher flow more capable of transporting more, and potentially larger, particles was expected. Interestingly, the SM trend in TSS concentration did not decrease as the spring season proceeded. Though COD and DOC were correlated in SM and not SP, this observation was reversed with respect to TSS, with COD and TSS correlated in SP ($R = 0.593$) but not SM ($R = 0.143$).

Larger, less chemically reactive particles remained within the SP, which is consistent with previous findings that large particles are deposited onsite and not transported with meltwater (Viklander 1999). The TSS likely experienced delayed releases from the SP after extended periods of warming melted the surface of the SP and transported those particles through the pack. This would also explain the relationship between TDS and TSS values at this site, where peaks in TSS concentration were observed in the days following TDS peaks (March 26th -March 29th, April 17th -April 20th, April 23rd -April 28th, all 2020 season). Relative to the preceding three sampling dates, elevated TSS was observed at Valley Rd. through April 28th, May 1st, and May 5th, 2020, though the concentration had dropped almost half by May 12th, 2020. Similar TSS behaviour was observed by Westerlund and Viklander (2011), who noted that over 90% of the metals burden in SPs was in particulate form and followed the same trends as TSS. It is possible the high TSS contained particulate COD, which has been previously observed in snow samples (Westerlund and Viklander 2011). Moreover, particulate COD tends to dissolve in meltwater (Viklander 1996), and some partial dissolution may explain the slightly higher variability in SM ($SD \pm 101$ mg/L) relative to snow ($SD \pm 79$ mg/L).

3.1.3 Metals and Polycyclic Aromatic Hydrocarbons (PAHs)

The average sum of measured metal species was 559 ± 187 $\mu\text{g/L}$ in SP and 725 ± 412 $\mu\text{g/L}$ in SM (Figure 2 with concentrations of individual elements included in Tables S9-S10). Concentrations of dissolved aluminum, iron, lead, and zinc were generally higher in SP samples, though SP concentrations were comparable to those in summer SW obtained as part of a parallel study (Popick et al. 2021). The largest overall contaminant peaks occurred in Valley Rd. SM on March 26th, 2020 (1,455 $\mu\text{g/L}$), April 17th, 2020 (1,988 $\mu\text{g/L}$) and April 23rd, 2020 (1,654 $\mu\text{g/L}$). All three of these contaminant peaks were accompanied by discharges of manganese measuring 575-919 $\mu\text{g/L}$. Other species-specific pulses in SP included aluminum at 401 $\mu\text{g/L}$ (Valley Rd., April 13th, 2019); arsenic at 26.2 $\mu\text{g/L}$ (Wanuske Rd., April 18th, 2019), copper at 135 $\mu\text{g/L}$ (USask, April 2nd, 2019), lead at 7.50 $\mu\text{g/L}$ (USask, April 24th, 2019), and selenium at 15.8 $\mu\text{g/L}$ (USask, April 2nd, 2019). In SM, species-specific pulses include mercury at 0.18 $\mu\text{g/L}$ (Central Ave, May 5th, 2020) and zinc at 581 $\mu\text{g/L}$ (Valley Rd, March 29th, 2020). In SP and SM samples from April 2nd, 2019 and March 7th, 2020, dissolved metal concentrations in SM were similar, but March 7th, 2020 SP concentrations were approximately 67% of those observed in April 2nd, 2019 SP.

While metals are naturally occurring geogenic elements, with their presence in sediments and soils predating industrialization (Owca et al. 2020), their mobilization in the urban environment can be markedly increased by human activities (Soto et al. 2011; Galfi et al. 2017; Sakson, et al. 2018). Metals may be present in SM in either dissolved or particulate forms with the dissolved metals being considered as bioavailable, and potentially toxic, to aquatic organisms. Chloride from winter road maintenance is a significant contributor to dissolved inorganic ligands in solution, thus enhancing the complexation of metals and increasing their dissolved concentration (Mayer et al. 2011a; Valtanen et al. 2014). Metals of particular concern due to their toxicity in SW, especially in cold climates, include lead, manganese, chromium, zinc, nickel, copper, and cadmium. At lower tropic levels, these metals can cause DNA damage, growth and biomass reduction, cellular respiration and enzyme dysfunction, inhibition of photosynthesis, and nervous system damage, among other adverse effects (Jaishankar et al. 2014; Zubala et al. 2017). In humans, arsenic, copper, lead, and zinc are associated with health effects including cancer, bone disease, hypertension, DNA and enzymatic dysfunction, nervous system damage, infertility, and organ failure (Chung et al. 2014; Ma et al. 2016; Zubala et al. 2017).

The average of measured dissolved Σ PAHs were 77 ± 157 $\mu\text{g/L}$ in SP and 0.587 ± 0.962 $\mu\text{g/L}$ in SM (Figure 3 with individual species in Table S11). Generally, dissolved PAHs in SP were 2 orders of magnitude greater than those detected in SM. With the exception of the

Valley Rd. April 24th, 2019 sample, at least 20 µg/L ΣPAHs were detected in all SP samples. SM samples typically contained < 2 µg/L ΣPAHs, with the exception of USask April 23rd, 2020 at 4.82 µg/L and Valley Rd. March 29th, 2020 at 1.14 µg/L. The most notable PAH discharge of 565 µg/L occurred in SP samples from Wanuskewin Rd. on April 13th, 2019, including notable discharges of pyrene, phenanthrene, and anthracene, while the largest pulses in SM occurred in Valley Rd. March 26th, 2020 (1.14 µg/L) and USask April 23rd, 2020 (4.82 µg/L) samples. Nearly all SP samples exceeded the CCME guidelines for fluorene, benzo[a]pyrene, pyrene, phenanthrene, and anthracene, while 50% of SM samples exceeded guideline thresholds for benzo[a]pyrene, pyrene and all except one exceeded the threshold for anthracene.

High concentrations of PAHs in SW are often correlated with high concentrations of heavy metals, indicating that roadways are also a major source of PAHs, mainly as vehicle exhaust, diesel soot, or from vehicle and pavement degradation (Aryal et al. 2010; Legret and Pagotto 1999; Moghadas et al. 2015). Considering that the Wanuskewin Rd. April 13th 2019 sample contained comparable DOC and COD to other April 13th, 2019 samples, its PAHs are likely traffic-derived. Sampling at this site did not disproportionately target contaminated snow relative to other sites or events; it is possible that oil-enriched particles were entrained in the sample and repartitioned into the dissolved phase when melted; however, previous observations of the same suite of PAHs noted 88-95% of species remained particle-bound in SW samples (Mayer et al. 2011b; Vijayan et al. 2019). This would be consistent with observations of preferential elution, in which the heavier and less polar compounds are the last to leave the SP. The April 13th, 2019 Wanuskewin Rd. sample may be the result of selecting a localized patch of pollution within the SP; even if this magnitude of pollution only occurred at one location onsite, the effluents may still be highly concentrated even after mixing. A pollution peak may also have been occurring at this site alone on the sampling day. The phenanthrene, pyrene, and anthracene found in this sample are likely compounds derived from coal tar, roadway degradation, and vehicle emissions which contribute the bulk of pollution in roadside snow banks (Kuoppamäki et al. 2014; Moghadas et al. 2015; Vijayan et al. 2019; Viklander 1999).

3.2 Toxicology Assessments

3.2.1 *R. subcapitata* Bioassay

Significant toxicity was generally not observed in either SP or SM samples, with the calculation of an EC₁₀ necessary to quantify toxic response for many samples (Table 2). It is assumed that chloride might have played a significant role in the osmotic stress experienced by *R. subcapitata*. While all samples inhibited growth at 100% concentration, few inhibited growth rates more than 50%. Furthermore, all serial dilutions below and including 50% often displayed stimulation instead of inhibition relative to the negative control. Toxicity did not seem related to any site-specific sample characteristics, though toxic responses were observed for all tested April 17th, 2020 samples. The most toxic response for which a 95% CI could be calculated was the USask SM sample on this date (EC₅₀ at 43.7 percent sample concentration; 95% CI 39.5-48.2). This sample most remarkably contains the highest dissolved copper discharge of all SM samples (Table S10). The April 17th, 2020 Central Ave. sample generated the second-lowest EC₅₀ threshold (54.3 percent sample concentration) but no CI could be calculated. This sample is not particularly remarkable compared to inter-event samples (the Valley Rd. site has higher TDS and chloride readings), inter-site samples (the April 23rd, 2020 Central Ave. sample has similar quality measurements but no detected EC₅₀), or the entire dataset (no contaminant spikes were measured in this sample). However, it does possess the greatest dissolved zinc concentration of any April 17th, 2020 sample (119 µg/L). These toxicity results seem to agree with previous observations that idiosyncratic sample mixtures are likely providing additive, synergistic, and antagonistic effects which cannot be attributed to a single species (Fulladosa et al. 2005; Tsiridis et al. 2006).

Table 2

72-hour growth inhibition EC_{50} and EC_{10} for *R. subcapitata* and 15-minute luminescence inhibition for *V. fischeri* (Microtox). Results are presented as percent of total sample concentration required to reach the endpoint. EC_{50} and EC_{10} values were generated using GraphPad Prism as a dose-response curve (see Methods) of, in the case of *R. subcapitata*, the initial ($t = 0$) fluorescence observed after 72 hours, and in the case of *V. fischeri*, the initial ($t = 0$) luminescence observed after 15 minutes. EC_{10} values were interpolated from relating 10% luminescence inhibition to sample concentration on a standardized curve (see Methods).

Year	Sample Date	Site Name	Algae		MicroTox	
			EC_{50} (CI 95%)	EC_{10} (CI 95%)	$EC_{50-15 \text{ min}}$ (CI 95%)	$EC_{10-15 \text{ min}}$ (CI 95%)
2019	April 2nd	USask (Snow)	103.4 (96.9-111.6)	28.1 (31.9-24.6)	54.0 (27.3-99.2)	53.4 (30.3-97.0)
		USask (SM)	ND	95.6 (50.3-NC)	54.4 (NC)	52.1 (29.0-96.7)
	April 18th	Valley Rd.	ND	36.8 (29.8-44.2)	56.5 (NC-68.3)	45.4 (33.7-49.6)
		Central Ave.	ND	62.0 (51.4-73.5)	43.6 (34.2-54.3)	36.0 (26.3-45.3)
		Wanuskewin Rd.	99.2 (94.8-104.1)	94.0 (66.8-NC)	55.1 (NC)	50.8 (36.1-79.7)
	April 24th	Valley Rd.	ND	NC	52.6 (NC)	49.9 (27.6-95.4)
USask		-	-	55.2 (42.4-72.0)	41.7 (28.4-70.5)	
2020	March 7th	Valley Rd. (Snow)	-	-	56.9 (NC)	54.9 (50.0-87.0)
		Valley Rd. (SM)	ND	33.5 (23.6-44.3)	59.5 (NC)	57.4 (44.3-91.8)
		USask (Snow)	ND	32.8 (24.1-42.2)	70.7 (NC)	71.1 (50.2-NC)
		USask (SM)	43.7 (39.5-48.2)	18.4 (14.9-22.7)	54.2 (NC)	52.0 (33.4-86.9)
	March 26th	Valley Rd.	ND	50.9 (35.7-65.3)	45.8 (35.8-56.8)	NC
	April 17th	Valley Rd.	123.2 (99.6-177.3)	38.7 (24.4-55.8)	91.2 (7.28-NC)	NC
		USask	96.4 (NC)	84.1 (49.9-158.3)	58.4 (NC)	55.4 (39.7-89.4)
		Central Ave.	54.3 (NC)	49.4 (28.9-93.2)	52.6 (49.8-NC)	50.8 (27.8-96.7)
		Wanuskewin Rd.	-	-	31.3 (21.7-44.2)	34.0 (23.9-50.8)
	April 23rd	Valley Rd.	-	-	ND	NC
		Central Ave.	ND	NC	1.19 (NC)	NC
	April 28th	Valley Rd.	-	-	0.062 (NC)	NC
		USask	-	-	NC	NC
	May 1st	Valley Rd.	-	-	58.4 (NC)	60.5 (50.2-96.9)
	May 5th	Central Ave.	-	-	99.9 (18.5-NC)	NC
May 12th	Valley Rd.	ND	90.7 (69.0-99.8)	56.8 (39.1-77.8)	45.9 (32.0-81.6)	

ND – not observable toxicity detected at the respective threshold; NC – not calculated.

Organic matter and TSS have been linked to acute toxicity as bound PAHs and metals cause mortality at acutely toxic concentrations and can cause adverse, potentially cumulative, effects at chronic concentrations (Barbosa et al. 2012; Glen and Sansalone 2002; Rossi et al. 2013). Concentrations of PAHs exceeding CCME guideline thresholds (see above) did not contribute to observable toxicity in SP over SM samples. This observation is not entirely unexpected, as Bragin et al. (2016) found PAHs did not contribute significant growth inhibition in *R. subcapitata*. Despite copper and zinc commonly causing toxicity in aquatic organisms (Babich and Stotzky 1978; Mayer et al. 2011b) alongside notable concentrations in the most toxic samples, no correlation between copper or zinc concentrations and algae toxicity was observed in this study ($R = 0.090$ and $R = 0.263$, respectively). As *R. subcapitata* can acclimate to aquatic concentrations between 0.5-100 $\mu\text{g Cu/L}$ (Bossuyt and Janssen 2005), local algae species may accommodate higher geogenic background levels. Brix et al. (2010) identified relatively low zinc toxicity risk for brief, one-hour events and relatively significant toxicity for chronic exposures, which could have toxicity implications for spring melt runoff from galvanized SW pipes. In cold climates, road salts can contribute significantly to toxicity and affect metal toxicity in winter and spring runoff. In a study examining the toxicity of

winter highway runoff, undiluted samples containing high road salt observed no survival in *D. magna*, *V. fischeri*, *Ceriodaphnia dubia*, or *Oncorhynchus mykiss* (Mayer et al. 2011 a). When testing the impact of the three road salts on rainbow trout, Hintz and Relyea (2017) found CaCl_2 was the most harmful to fish growth, followed by NaCl and then MgCl_2 . Conversely, emphasizing the intraspecies variability of toxicity, Hopkins et al. (2013) found MgCl_2 and NaCl caused comparable developmental deformities in rough-skinned newts.

3.3.2 *V. fischeri* Bioassay

Similar to *R. subcapitata*, displayed some degree of luminescence inhibition in samples at 100% concentration (Table 2). However, inhibition was not detected in all samples and stimulation relative to the negative control was often observed in serial dilutions. No remarkable site- or event-related trends in toxicity were observed, though the survival rates in diluted sample wells created difficulties in calculating IC_{50} with 95% CI for many samples. The April 23rd, 2020 Valley Rd. sample displayed the highest toxic potential (15-min IC_{50} = 8.3% sample concentration); this pulse notably had the highest concentration of dissolved manganese (919 $\mu\text{g/L}$) and the second-highest concentrations of dissolved mercury (0.15 $\mu\text{g/L}$) and chloride (2,900 mg/L).

Fulladosa et al. (2005) found metals to be toxic to *V. fischeri* in the order of mercury > silver > copper > zinc, while cobalt, cadmium, chromium(VI), arsenic(V), and arsenic(III) showed no significant toxicity. However, in this study, as with algae, no significant correlations were noted between dissolved metals and toxic response. Moderate correlations were found between toxicity and chromium ($R = 0.453$), manganese ($R = 0.480$), nickel ($R = 0.479$), and strontium ($R = 0.354$). In testing binary mixtures of metals, Fulladosa et al. (2005) found copper-zinc mixtures to be additive, while Tsiridis et al. (2006) observed a synergistic effect. Interestingly, the latter comments that all copper-zinc IC_{50} results differed significantly from theoretical predictions; when combined with mixtures of humic acids, the toxicity of the solution decreased relative to the metals-only mixture. Interestingly, most of the aforementioned metal species were found to be significantly correlated with chloride concentrations (see Section 3.1). The complexity of sample mixture is potentially reflected in these results. Chloride concentrations have been implicated as the dominant driver in SM toxicity relative to metals and PAHs (Mayer et al. 2011a; Prosser et al. 2017), they appear to have increased the influence of select metals on toxicity, as previously observed (Bäckström et al. 2004; Reinosdotter and Viklander 2007). However, despite the impact which would be expected from, for example, the Valley Rd. March 26th, 2020 (5,800 mg/L chloride) or the April 23rd, 2020 sample (2,900 mg/L chloride, 919 $\mu\text{g/L}$ manganese; 0.15 $\mu\text{g/L}$ mercury), none was observed. That antagonistic mechanisms against chloride or metal toxicity seem apparent in samples is most easily indicated by comparing *R. subcapitata* and *V. fischeri* data: EC_{50} thresholds for algae often occurred at greater sample concentrations, though algae should be more susceptible to salt toxicity relative to *V. fischeri* (Cook et al. 2000). Previous studies which found significant salt toxicity sampled winter road runoff in the Ontario (Mayer et al. 2011a; Prosser et al. 2017). Though carbonate-rich soils are local to the Saskatoon area, with the CoS reporting a river water hardness of 191 $\text{mg CaCO}_3/\text{L}$ on the municipal website, Prosser et al. found 3,159 mg/L of chloride impacted 50% mortality in freshwater mussels (*Lampsilis siliquoidea*) at a water hardness of 237 $\text{mg CaCO}_3/\text{L}$ (Prosser et al. 2017). As local water hardness therefore would explain the lack of toxic chloride impact in this study, it is probable that the aging of SPs and its onsite SM puddles alter their toxic potential relative to fresh road runoff.

3.4 Land use management

To estimate the quantity of snow at CoS facilities prior to the melt season, UAS-LIDAR imagery of the Valley Rd. facility was obtained on March 13th, 2020 with a snow estimate of 151,910 m^3 . Assuming the Valley Rd. facility receives half of the CoS's plowed snow (*pers. comm.*), a city-wide facility volume of approximately 300,000 m^3 was obtained. Using a sample taken from Valley Rd., a SP density of approximately 520 kg/m^3 was determined which was then used in conjunction with a water density of 1,000 kg/m^3 to produce an estimate of 79,000 m^3 in SWE for the Valley Rd. site and 34,500 m^3 at each of CoS other facilities. Similarly, the USask site snow volume was estimated and the SWE determined to be 10,000 m^3 . Assuming these volumes were discharged to the environment through the melt season, the 2020 seasonal loading estimate was calculated using the average measured concentration of TDS, TSS, COD, DOC, copper, chromium, manganese, nickel, lead, selenium, zinc, and ΣPAHs (Table 3). It should be noted that this loading is representative of CoS traffic-related surfaces, however, SM runoff within catchments is likely to follow the same transport paths as SW. However, contaminant concentrations in this non-road snow were not determined in the current study. As 35-85% of SM has been observed to infiltrate on the Canadian Prairies, even over frozen soils (Mohammed et al. 2019), it is not unreasonable to assume roadside SPs (which would discharge directly to storm sewers if not removed) account for a significant portion of urban contamination in snow-derived runoff.

Given it is the largest snow storage facility, as expected the Valley Rd. site contributed the highest calculated loadings for all parameters shown in Table 3. This includes exceptionally high values for TDS (169,231 kg), COD (24,524 kg), and DOC (611 kg). Interestingly, the

TSS loadings for the three CoS sites were all in a similar range (30,000 to 40,000 kg) despite having significant snow volume differences. However, this could be attributed to soil erosion on the smaller sites given the Valley Rd. site is the only facility contained on a concrete surface. This is also likely the reason why the TDS loading was very high at the Valley Rd. facility as there is no opportunity for infiltration as available at other sites. The TDS and COD were strongly correlated ($R = 0.962$) as were the COD and DOC ($R = 0.966$). Organics were not significantly present in snow with DOC comprising 0.36-1.03% of TDS loading. Two sites contributed 89% of DOC loading: Valley Rd. (611 kg) and Central Ave. (199 kg). Strong correlations were also observed between COD loading and copper ($R = 0.918$), chromium ($R = 0.980$), nickel ($R = 0.973$), zinc ($R = 0.958$), and Σ PAHs ($R = 0.953$) along with a moderate correlation in lead ($R = 0.948$). The largest metal loading estimates were of manganese (25 kg) and zinc (12 kg) driven by single-event pulses observed at Valley Rd. The next highest loading estimates were copper (2.25 kg with 52% comprising Valley Rd.) and nickel (1.38 kg with 64% comprising Valley Rd.). Loading estimates for copper, manganese, selenium, and Σ PAHs were not found to be significantly correlated to snow volume, though correlations were observed for chromium ($R = 0.974$), nickel ($R = 0.945$), lead ($R = 0.921$), and zinc ($R = 0.950$). However, each site's characteristics are quite variable making direct comparisons difficult and potentially erroneous. For example, the TDS, COD, and DOC values at the Central Ave. site were markedly higher than the Wanuskewin Rd. despite each have the same estimated SWE volume.

During the winter in cold-region Canadian cities, precipitation falls as snow and runoff events do not occur for several months, though winter activities continue in the catchment. After a snowfall event, municipalities will plow snow from the roads into roadside banks and apply grit material (road salt or sand). Within hours of deposition, these snowbanks become contaminant sinks for heavy metals and particulates from traffic and winter maintenance activities, as well as transformation products of primarily organic contaminants (Glen and Sansalone 2002; Sillanpää and Koivusalo 2013; Westerlund and Viklander 2011). In this study, while sample DOC contributed to oxygen demand, the majority of COD is likely inorganic: COD has been observed as a major source of contamination in roadway runoff (Huang et al. 2007) and it is not unreasonable that COD in snow would be mainly traffic-derived. Strong COD correlations with reactive metals species Cr, Ni, Pb, and Zn indicate probable road and vehicle origins. However, despite all snow facilities receiving a mixture of roadside snow, the estimated contaminant loads for each facility varied. Contaminant deposition decreases drastically with increased distance from the roadway, with the bulk of pollutants deposited immediately beside the road (Hautala et al. 1995; Kuoppamäki et al. 2014). Hautala et al. (1995) observed chloride concentrations were significantly greater at 10 m than 30 m from the road edge while the opposite was true for low-molecular-weight (LMW) polyaromatic hydrocarbons (PAHs). Industrial emissions have additionally been implicated in non-roadside SP contamination (Li et al. 2015). The comparatively low PAH (0.07 kg) to DOC loads (907 kg) are likely due to high particle affinity, but deposition distribution may play some role in inter-site variation. Facilities likely received volumes of non-roadside snow which contributed different contaminant species and concentrations. The Valley Rd. site possessed the greatest contamination load as expected due to lack of on-site infiltration. However, its TSS values were comparable to those observed at facilities with half the estimated SM volume at Wanuskewin Rd. and Central Ave. The Central Ave. site possessed 89-fold higher TDS and 70-fold higher COD than the Wanuskewin Rd. site despite seemingly similar environmental characteristics. The infiltration capacity at the Central Ave site may have been reduced by high-TDS SM runoff over time, resulting in overall poorer SM quality leaving the site and impacting surrounding environments.

4.0 Conclusions

The main objective of this study was to assess urban SM quality from storage facilities. Comprehensive analysis of conventional SW parameters and toxicological results for *R. subcapitata* and *V. fischeri* determined herein have contributed to the limited database for urban SP and SM runoff worldwide. Snow stored at urban facilities is primarily roadside snow, while cold-climate SW studies largely analyze winter road runoff; therefore, this data may reflect conditions experienced in roadside snowpacks, or conditions in aged SM, relative to fresh winter road runoff. Nevertheless, quality data from snow storage facilities is lacking, though previous research has shown the roadside snow taken to these facilities contribute a significant portion of the traffic contaminant burden. As SPs provide an intermediary for the transport of urban SW contaminants to receiving environments, SP treatment strategies must be developed to ensure proper contaminant removals before releasing into receiving environments.

Observations were generally in agreement with previous literature, with preferential elution of TDS out of the SP as the melt period commenced and contaminant spikes observed following warm, sunny days. Significant chloride and manganese peaks occurred throughout the 2020 melt season, indicating management facilities must manage melt periods featuring contaminant spikes. Though fluctuating, elevated TSS values persisted in SPs and elevated TDS persisted in snowmelt weeks into the spring melt season, indicative of pulsed melt events instead of an elevated baseline throughout the melt period. Increasing thaw-freeze periods may introduce

contaminant spikes during winter months as well, extending the melt period requiring attention. Despite the magnitude of contamination reported in certain samples, no significant toxicological trends were observed in either *R. subcapitata* or *V. fischeri*.

It is estimated that snow plowed from CoS roads in 2020 contributed a total of 226,000 kg TSS and 119,000 kg TDS at their outlets. A majority (60%) of this loading undergoes primary treatment at the Valley Rd. facility and the true quality impacting the SSR is yet unknown. Simple contaminant loading calculations using seasonal mean concentrations indicate relatively high TDS and relatively low TSS in snowmelt runoff at the paved Valley Rd. facility. This may indicate infiltration of TDS and erosion of TSS at unpaved sites, though research into on-site soil quality is needed. The traffic-derived COD is strongly correlated with chromium, nickel, lead, and zinc. However, the lack of continuous flow-measurement data at snow facilities limits the ability to calculate flow-weighted site mean concentrations and only a seasonal mean loading estimate could be ascertained from the data. Furthermore, no snowfall depth-SP volume correlations could be calculated due to limited data. This study establishes foundations upon which the aforementioned data can be developed.

Declarations

Acknowledgements

Markus Brinkmann is currently a faculty member of the Global Water Futures (GWF) program, which received funds from the Canada First Research Excellence Funds (CFREF). The authors would like to acknowledge the Natural Sciences and Engineering Research Council of Canada (NSERC) for funding this research through an Engage Grant (M.B.) and Discovery Grant (K.M.). That authors are also grateful for in-kind support from the City of Saskatoon, specifically through the active involvement of the following individuals: Mitchell McMann, Angela Schmidt, Hossein Azinfar, Sudhir Pandey, and Grant Gardner.

Ethical Approval

Not applicable

Consent to Participate

Not applicable

Consent to Publish

Not applicable

Authors Contributions

HP completed all research fieldwork and sample analyses. MB and KM assisted with conceptualization of sampling regime and methods, while also acquired necessary funding for the research. All authors contributed to the manuscript writing and editing, and have read and approved the final manuscript.

Competing Interests

The authors declare that they have no competing interests.

Availability of data and materials

Not applicable.

References

1. Al Masum A, Bettman N, Read S, Hecker M, Brinkmann M, McPhedran K Urban stormwater runoff pollutant loadings: GIS land use classification vs. sample-based predictions. Submitted to Environ Sci Pollut Res ESPR-D-21-12380.
2. Albert MR, Hardy JP (1995) Ventilation experiments in a seasonal snow cover. Biogeochem Seas snow-covered catchments Proc Symp Boulder, 1995 41–49

3. Aryal R, Vigneswaran S, Kandasamy J, Naidu R (2010) Urban stormwater quality and treatment. *Korean J Chem Eng* 27:1343–1359. <https://doi.org/10.1007/s11814-010-0387-0>
4. Babich H, Stotzky G (1978) Toxicity of zinc to fungi, bacteria, and coliphages: Influence of chloride ions. *Appl Environ Microbiol* 36:906–914
5. Bäckström M, Karlsson S, Bäckman L, Folkesson L, Lind B (2004) Mobilisation of heavy metals by deicing salts in a roadside environment. *Water Res* 38:720–732. <https://doi.org/10.1016/j.watres.2003.11.006>
6. Barbosa AE, Fernandes JN, David LM (2012) Key issues for sustainable urban stormwater management. *Water Res* 46:6787–6798. <https://doi.org/10.1016/j.watres.2012.05.029>
7. Bartlett AJ, Rochfort Q, Brown LR, Marsalek J (2012) Causes of toxicity to *Hyalella azteca* in a stormwater management facility receiving highway runoff and snowmelt. Part I: Polycyclic aromatic hydrocarbons and metals. *Sci Total Environ* 414:227–237. <https://doi.org/10.1016/j.scitotenv.2011.11.041>
8. Blecken GT, Rentz R, Malmgren C, Öhlander B, Viklander M (2012) Stormwater impact on urban waterways in a cold climate: Variations in sediment metal concentrations due to untreated snowmelt discharge. *J Soils Sediments* 12:758–773. <https://doi.org/10.1007/s11368-012-0484-2>
9. Bossuyt BTA, Janssen CR (2005) Copper regulation and homeostasis of *Daphnia magna* and *Pseudokirchneriella subcapitata*: Influence of acclimation. *Environ Pollut* 136:135–144. <https://doi.org/10.1016/j.envpol.2004.11.024>
10. Brix K V, Keithly J, Santore RC, DeForest DK, Tobiasson S (2010) Ecological risk assessment of zinc from stormwater runoff to an aquatic ecosystem. *Sci Total Environ* 408:1824–1832. <https://doi.org/10.1016/j.scitotenv.2009.12.004>
11. Calonne N, Flin F, Morin S, Lesaffre B, Du Roscoat SR, Geindreau C (2011) Numerical and experimental investigations of the effective thermal conductivity of snow. *Geophys Res Lett* 38:1–21. <https://doi.org/10.1029/2011GL049234>
12. Calonne N, Geindreau C, Flin F, Morin S, Lesaffre B, Rolland Du Roscoat S, Charrier P (2012) 3-D image-based numerical computations of snow permeability: Links to specific surface area, density, and microstructural anisotropy. *Cryosphere* 6:939–951. <https://doi.org/10.5194/tc-6-939-2012>
13. Challis, JK, Popick H, Prajapati S, Harder P, Giesy JP, McPhedran K, Brinkmann (2021) Occurrences of tire rubber-derived contaminants in cold-climate urban runoff. *Environ Sci Technol Letters* <https://doi.org/10.1021/acs.estlett.1c00682>
14. Chung JY, Yu S Do, Hong YS (2014) Environmental source of arsenic exposure. *J Prev Med Public Heal* 47:253–257. <https://doi.org/10.3961/jpmph.14.036>
15. Codling G, Yuan H, Jones PD, Giesy JP, Hecker M (2020) Metals and PFAS in stormwater and surface runoff in a semi-arid Canadian city subject to large variations in temperature among seasons. *Environ Sci Pollut Res* 27:18232–18241. <https://doi.org/10.1007/s11356-020-08070-2>
16. Cook S V, Chu A, Goodman RH (2000) Influence of salinity on *Vibrio fischeri* and lux-modified *Pseudomonas fluorescens* toxicity bioassays. *Environ Toxicol Chem* 19:2474–2477. <https://doi.org/10.1002/etc.5620191012>
17. Ebner PP, Schneebeli M, Steinfeld A (2016) Metamorphism during temperature gradient with undersaturated advective airflow in a snow sample. *Cryosphere* 10:791–797. <https://doi.org/10.5194/tc-10-791-2016>
18. Environment Canada (1993) Biological test method. Toxicity test using luminescent bacteria
19. EPA (Institution/Organization) (2002) Method 1003.0: Green Alga, *Selenastrum capricornutum*, Growth Test; Chronic Toxicity
20. Exall K, Marsalek J, Rochfort Q, Kydd S (2011a) Chloride transport and related processes at a municipal snow storage and disposal site. *Water Qual Res J Canada* 46:148–156. <https://doi.org/10.2166/wqrjc.2011.023>
21. Exall K, Rochfort Q, Marsalek J (2011b) Measurement of cyanide in urban snowmelt and runoff. *Water Qual Res J Canada* 46:137–147. <https://doi.org/10.2166/wqrjc.2011.022>
22. Fulladosa E, Murat JC, Martínez M, Villaescusa I (2005a) Patterns of metals and arsenic poisoning in *Vibrio fischeri* bacteria. *Chemosphere* 60:43–48. <https://doi.org/10.1016/j.chemosphere.2004.12.026>
23. Fulladosa E, Murat JC, Villaescusa I (2005b) Study on the toxicity of binary equitoxic mixtures of metals using the luminescent bacteria *Vibrio fischeri* as a biological target. *Chemosphere* 58:551–557. <https://doi.org/10.1016/j.chemosphere.2004.08.007>
24. Galfi H, Österlund H, Marsalek J, Viklander M (2017) Mineral and Anthropogenic Indicator Inorganics in Urban Stormwater and Snowmelt Runoff: Sources and Mobility Patterns. *Water Air Soil Pollut* 228. <https://doi.org/10.1007/s11270-017-3438-x>
25. Glen DW, Sansalone JJ (2002) Accretion and partitioning of heavy metals associated with snow exposed to urban traffic and winter storm maintenance activities. II. *J Environ Eng* 128:167–185. [https://doi.org/10.1061/\(ASCE\)0733-9372\(2002\)128:2\(167\)](https://doi.org/10.1061/(ASCE)0733-9372(2002)128:2(167))

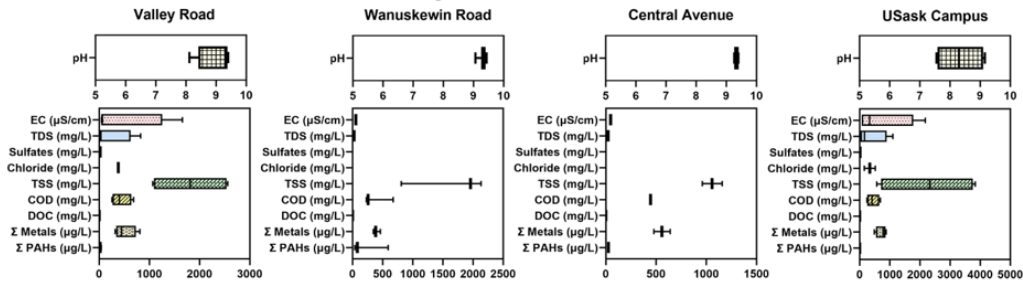
26. HACH (2014) Chemical oxygen demand, dichromate method. Hach DOC316.53.:10. <https://doi.org/10.1002/9780470114735.hawley03365>
27. Hautala EL, Rekilä R, Tarhanen J, Ruuskanen J (1995) Deposition of motor vehicle emissions and winter maintenance along roadside assessed by snow analyses. *Environ Pollut* 87:45–49. [https://doi.org/10.1016/S0269-7491\(99\)80006-2](https://doi.org/10.1016/S0269-7491(99)80006-2)
28. Helmreich B, Hilliges R, Schriewer A, Horn H (2010) Runoff pollutants of a highly trafficked urban road - Correlation analysis and seasonal influences. *Chemosphere* 80:991–997. <https://doi.org/10.1016/j.chemosphere.2010.05.037>
29. Hengren L, Goonetilleke A, Ayoko GA, Mostert MMM (2010) Distribution of polycyclic aromatic hydrocarbons in urban stormwater in Queensland, Australia. *Environ Pollut* 158:2848–2856. <https://doi.org/10.1016/j.envpol.2010.06.015>
30. Hintz WD, Relyea RA (2017) Impacts of road deicing salts on the early-life growth and development of a stream salmonid: Salt type matters. *Environ Pollut* 223:409–415. <https://doi.org/10.1016/j.envpol.2017.01.040>
31. Hopkins GR, French SS, Brodie ED (2013) Increased frequency and severity of developmental deformities in rough-skinned newt (*Taricha granulosa*) embryos exposed to road deicing salts (NaCl & MgCl₂). *Environ Pollut* 173:264–269. <https://doi.org/10.1016/j.envpol.2012.10.002>
32. Howitt JA, Mondon J, Mitchell BD, Kidd T, Eshelman B (2014) Urban stormwater inputs to an adapted coastal wetland: Role in water treatment and impacts on wetland biota. *Sci Total Environ* 485–486:534–544. <https://doi.org/10.1016/j.scitotenv.2014.03.101>
33. Huang J, Du P, Ao C, Ho M, Lei M, Zhao D, Wang Z (2007) Multivariate analysis for stormwater quality characteristics identification from different urban surface types in Macau. *Bull Environ Contam Toxicol* 79:650–654. <https://doi.org/10.1007/s00128-007-9297-1>
34. Jaishankar M, Tseten T, Anbalagan N, Mathew BB, Beeregowda KN (2014) Toxicity, mechanism and health effects of some heavy metals. *Interdiscip Toxicol* 7:60–72. <https://doi.org/10.2478/intox-2014-0009>
35. Karlavičiene V, Švediene S, Marčiulioniene DE, Randerson P, Rimeika M, Hogland W (2009) The impact of storm water runoff on a small urban stream. *J Soils Sediments* 9:6–12. <https://doi.org/10.1007/s11368-008-0038-9>
36. Kuchta SL, Cessna AJ (2009) Fate of lincomycin in snowmelt runoff from manure-amended pasture. *Chemosphere* 76:439–446. <https://doi.org/10.1016/j.chemosphere.2009.03.069>
37. Kuoppamäki K, Setälä H, Rantalainen AL, Kotze DJ (2014) Urban snow indicates pollution originating from road traffic. *Environ Pollut* 195:56–63. <https://doi.org/10.1016/j.envpol.2014.08.019>
38. Lazur A, VanDerwerker T, Koepenick K (2020) Review of Implications of Road Salt Use on Groundwater Quality—Corrosivity and Mobilization of Heavy Metals and Radionuclides. *Water Air Soil Pollut* 231:. <https://doi.org/10.1007/s11270-020-04843-0>
39. LeBoutillier DW, Kells JA, Putz GJ (2000) Prediction of pollutant load in stormwater runoff from an urban residential area. *Can Water Resour J* 25:343–359. <https://doi.org/10.4296/cwrj2504343>
40. Legret M, Pagotto C (1999) Evaluation of pollutant loadings in the runoff waters from a major rural highway. *Sci Total Environ* 235:143–150. [https://doi.org/10.1016/S0048-9697\(99\)00207-7](https://doi.org/10.1016/S0048-9697(99)00207-7)
41. Li X, Jiang F, Wang S, Turdi M, Zhang Z (2015) Spatial distribution and potential sources of trace metals in insoluble particles of snow from Urumqi, China. *Environ Monit Assess* 187:. <https://doi.org/10.1007/s10661-014-4144-4>
42. Löwe H, Spiegel JK, Schneebeli M (2011) Interfacial and structural relaxations of snow under isothermal conditions. *J Glaciol* 57:499–510. <https://doi.org/10.3189/002214311796905569>
43. Ma Y, Egodawatta P, McGree J, Liu A, Goonetilleke A (2016) Human health risk assessment of heavy metals in urban stormwater. *Sci Total Environ* 557–558:764–772. <https://doi.org/10.1016/j.scitotenv.2016.03.067>
44. Matos C, Bento R, Bentes I (2015) Urban Land-Cover, Urbanization Type and Implications for Storm Water Quality: Vila Real as a Case Study. *J Hydrogeol Hydrol Eng* 04: <https://doi.org/10.4172/2325-9647.1000122>
45. Mayer T, Rochfort Q, Marsalek J, Parrott J, Servos M, Baker M, Mcinnis R, Jurkovic A, Scott I (2011a) Environmental characterization of surface runoff from three highway sites in Southern Ontario, Canada: 2. Toxicology. *Water Qual Res J Canada* 46:121–136. <https://doi.org/10.2166/wqrjc.2011.036>
46. Mayer T, Rochfort Q, Marsalek J, Parrott J, Servos M, Baker M, Mcinnis R, Jurkovic A, Scott I (2011b) Environmental characterization of surface runoff from three highway sites in Southern Ontario, Canada: 1. Chemistry. *Water Qual Res J Canada* 46:110–120. <https://doi.org/10.2166/wqrjc.2011.035>
47. Mayer T, Snodgrass WJ, Morin D (1999) Spatial Characterization of the Occurrence of Road Salts and Their Environmental Concentrations as Chlorides in Canadian Surface Waters and Benthic Sediments. *Water Qual Res J Canada* 34:545–574

48. McLaren RR (1982) Sampling of Snowpacks for Chemical Analysis in Southwestern British Columbia. Vancouver, Canada
49. McLeod SM, Kells JA, Putz GJ (2006) Urban runoff quality characterization and load estimation in Saskatoon, Canada. *J Environ Eng* 132:1470–1481. [https://doi.org/10.1061/\(ASCE\)0733-9372\(2006\)132:11\(1470\)](https://doi.org/10.1061/(ASCE)0733-9372(2006)132:11(1470))
50. Meland S, Borgström R, Heier LS, Rosseland BO, Lindholm O, Salbu B (2010) Chemical and ecological effects of contaminated tunnel wash water runoff to a small Norwegian stream. *Sci Total Environ* 408:4107–4117. <https://doi.org/10.1016/j.scitotenv.2010.05.034>
51. Moghadas S, Gustafsson AM, Muthanna TM, Marsalek J, Viklander M (2016) Review of models and procedures for modelling urban snowmelt. *Urban Water J* 13:396–411. <https://doi.org/10.1080/1573062X.2014.993996>
52. Moghadas S, Paus KH, Muthanna TM, Herrmann I, Marsalek J, Viklander M (2015) Accumulation of Traffic-Related Trace Metals in Urban Winter-Long Roadside Snowbanks. *Water Air Soil Pollut* 226:1–15. <https://doi.org/10.1007/s11270-015-2660-7>
53. Mohammed AA, Pavlovskii I, Cey EE, Hayashi M (2019) Effects of preferential flow on snowmelt partitioning and groundwater recharge in frozen soils. *Hydrol Earth Syst Sci* 23:5017–5031. <https://doi.org/10.5194/hess-23-5017-2019>
54. Murphy LU, O'Sullivan A, Cochrane TA (2014) Quantifying the spatial variability of airborne pollutants to stormwater runoff in different land-use catchments. *Water Air Soil Pollut* 225:. <https://doi.org/10.1007/s11270-014-2016-8>
55. Oberts GL, Marsalek J, Viklander M (2000) Review of Water Quality Impacts of Winter Operation of Urban Drainage. *Water Qual Res J Canada* 35:781–808
56. Owca TJ, Kay ML, Faber J, Remmer CR, Zabel N, Wiklund JA, Wolfe BB, Hall RI (2020) Use of pre-industrial baselines to monitor anthropogenic enrichment of metals concentrations in recently deposited sediment of floodplain lakes in the Peace-Athabasca Delta (Alberta, Canada). *Environ Monit Assess* 192:. <https://doi.org/10.1007/s10661-020-8067-y>
57. Pavlovskii I, Hayashi M, Itenfisu D (2019) Midwinter melts in the Canadian prairies: Energy balance and hydrological effects. *Hydrol Earth Syst Sci* 23:1867–1883. <https://doi.org/10.5194/hess-23-1867-2019>
58. Popick, H., Brinkmann, M., McPhedran, K. (2021) Assessment of stormwater discharge contamination and toxicity for a cold-climate urban landscape. Submitted to *Env Sci Europe ESEU-D-21-00173*.
59. Prosser RS, Rochfort Q, McInnis R, Exall K, Gillis PL (2017) Assessing the toxicity and risk of salt-impacted winter road runoff to the early life stages of freshwater mussels in the Canadian province of Ontario. *Environ Pollut* 230:589–597. <https://doi.org/10.1016/j.envpol.2017.07.001>
60. Qinqin L, Qiao C, Jiancai D, Weiping H (2015) The use of simulated rainfall to study the discharge process and the influence factors of urban surface runoff pollution loads. *Water Sci Technol* 72:484–490. <https://doi.org/10.2166/wst.2015.239>
61. Reinosdotter K, Viklander M (2007) Road salt influence on pollutant releases from melting urban snow. *Water Qual Res J Canada* 42:153–161. <https://doi.org/10.2166/wqrj.2007.019>
62. Rentz R, Widerlund A, Viklander M, Öhlander B (2011) Impact of urban stormwater on sediment quality in an enclosed bay of the Lule river, Northern Sweden. *Water Air Soil Pollut* 218:651–666. <https://doi.org/10.1007/s11270-010-0675-7>
63. Rossi L, Chèvre N, Fankhauser R, Margot J, Curdy R, Babut M, Barry DA (2013) Sediment contamination assessment in urban areas based on total suspended solids. *Water Res* 47:339–350. <https://doi.org/10.1016/j.watres.2012.10.011>
64. Sakson G, Brzezinska A, Zawilski M (2018) Emission of heavy metals from an urban catchment into receiving water and possibility of its limitation on the example of Lodz city. *Environ Monit Assess* 190:. <https://doi.org/10.1007/s10661-018-6648-9>
65. Sanzo D, Hecnar SJ (2006) Effects of road de-icing salt (NaCl) on larval wood frogs (*Rana sylvatica*). *Environ Pollut* 140:247–256. <https://doi.org/10.1016/j.envpol.2005.07.013>
66. Schrimpff E, Thomas W, Herrmann R (1979) Regional patterns of contaminants (PAH, pesticides and trace metals) in snow of Northeast Bavaria and their relationship to human influence and orographic effects. *Water Air Soil Pollut* 11:481–497. <https://doi.org/10.1007/BF00283439>
67. Shotyk W, Krachler M, Aeschbach-Hertig W, Hillier S, Zheng J (2010) Trace elements in recent groundwater of an artesian flow system and comparison with snow: Enrichments, depletions, and chemical evolution of the water. *J Environ Monit* 12:208–217. <https://doi.org/10.1039/b909723f>
68. Sillanpää N, Koivusalo H (2013) Catchment-scale evaluation of pollution potential of urban snow at two residential catchments in southern Finland. *Water Sci Technol* 68:2164–2170. <https://doi.org/10.2166/wst.2013.466>
69. Sillanpää N, Koivusalo H (2015) Impacts of urban development on runoff event characteristics and unit hydrographs across warm and cold seasons in high latitudes. *J Hydrol* 521:328–340. <https://doi.org/10.1016/j.jhydrol.2014.12.008>

70. Soto P, Gaete H, Hidalgo ME (2011) Evaluación de la actividad de la catalasa, peroxidación lipídica, clorofila-a y tasa de crecimiento en la alga verde de agua dulce *Pseudokirchneriella subcapitata* expuesta a cobre y zinc. *Lat Am J Aquat Res* 39:280–285. <https://doi.org/10.3856/vol39-issue2-fulltext-9>
71. Taka M, Aalto J, Virkanen J, Luoto M (2016) The direct and indirect effects of watershed land use and soil type on stream water metal concentrations. *Water Resour Res* 52:. <https://doi.org/10.1002/2016WR019226>
72. Taka M, Kokkonen T, Kuoppamäki K, Niemi T, Sillanpää N, Valtanen M, Warsta L, Setälä H (2017) Spatio-temporal patterns of major ions in urban stormwater under cold climate. *Hydrol Process* 31:1564–1577. <https://doi.org/10.1002/hyp.11126>
73. Tsiroidis V, Petala M, Samaras P, Hadjispyrou S, Sakellaropoulos G, Kungolos A (2006) Interactive toxic effects of heavy metals and humic acids on *Vibrio fischeri*. *Ecotoxicol Environ Saf* 63:158–167. <https://doi.org/10.1016/j.ecoenv.2005.04.005>
74. Valeo C, Ho CLI (2004) Modelling urban snowmelt runoff. *J Hydrol* 299:237–251. <https://doi.org/10.1016/j.jhydrol.2004.08.007>
75. Valtanen M, Sillanpää N, Setälä H (2014) The effects of urbanization on runoff pollutant concentrations, loadings and their seasonal patterns under cold climate. *Water Air Soil Pollut* 225:. <https://doi.org/10.1007/s11270-014-1977-y>
76. Vijayan A, Österlund H, Marsalek J, Viklander M (2019) Laboratory Melting of Late-Winter Urban Snow Samples: The Magnitude and Dynamics of Releases of Heavy Metals and PAHs. *Water Air Soil Pollut* 230:. <https://doi.org/10.1007/s11270-019-4201-2>
77. Vijayan A, Österlund H, Marsalek J, Viklander M (2021) Estimating Pollution Loads in Snow Removed from a Port Facility: Snow Pile Sampling Strategies. *Water, Air, Soil Pollut* 232:. <https://doi.org/10.1007/s11270-021-05002-9>
78. Viklander M (1996) Urban snow deposits - Pathways of pollutants. *Sci Total Environ* 189–190:379–384. [https://doi.org/10.1016/0048-9697\(96\)05234-5](https://doi.org/10.1016/0048-9697(96)05234-5)
79. Viklander M (1999) Substances in urban snow. A comparison of the contamination of snow in different parts of the city of Lulea, Sweden. *Water Air Soil Pollut* 114:377–394. <https://doi.org/10.1023/A:1005121116829>
80. Westerlund C, Viklander M (2006) Particles and associated metals in road runoff during snowmelt and rainfall. *Sci Total Environ* 362:143–156. <https://doi.org/10.1016/j.scitotenv.2005.06.031>
81. Westerlund C, Viklander M (2008) Transport of total suspended solids during snowmelt - Influence by road salt, temperature and surface slope. *Water Air Soil Pollut* 192:3–10. <https://doi.org/10.1007/s11270-007-9579-6>
82. Westerlund C, Viklander M (2011) Pollutant release from a disturbed urban snowpack in northern Sweden. *Water Qual Res J Canada* 46:98–109. <https://doi.org/10.2166/wqrjc.2011.025>
83. Westerlund C, Viklander M, Hernebring C, Svensson G (2008) Modelling sediment transport during snowmelt- and rainfall-induced road runoff. *Hydrol Res* 39:113–122. <https://doi.org/10.2166/nh.2008.040>
84. White PA, Rasmussen JB, Blaise C (1995) Genotoxicity of snow in the Montreal metropolitan area. *Water Air Soil Pollut* 83:315–334
85. Yang YY, Toor GS (2017) Sources and mechanisms of nitrate and orthophosphate transport in urban stormwater runoff from residential catchments. *Water Res* 112:176–184. <https://doi.org/10.1016/j.watres.2017.01.039>
86. Zgheib S, Moilleron R, Chebbo G (2008) Screening of priority pollutants in urban stormwater: Innovative methodology. *WIT Trans Ecol Environ* 111:235–244. <https://doi.org/10.2495/WP080231>
87. Zinger I, Delisle CE (1988) Quality of Used-Snow Discharged in the St-Lawrence River. *Water Air Soil Pollut* 39:47–57
88. Zubala T, Patro M, Boguta P (2017) Variability of zinc, copper and lead contents in sludge of the municipal stormwater treatment plant. *Environ Sci Pollut Res* 24:17145–17152. <https://doi.org/10.1007/s11356-017-9338-1>
89. (2018) 2540 SOLIDS. In: *Standard Methods For the Examination of Water and Wastewater*. American Public Health Association

Figures

Snow Pile: Physicochemical Characteristics



Snowmelt: Physicochemical Characteristics

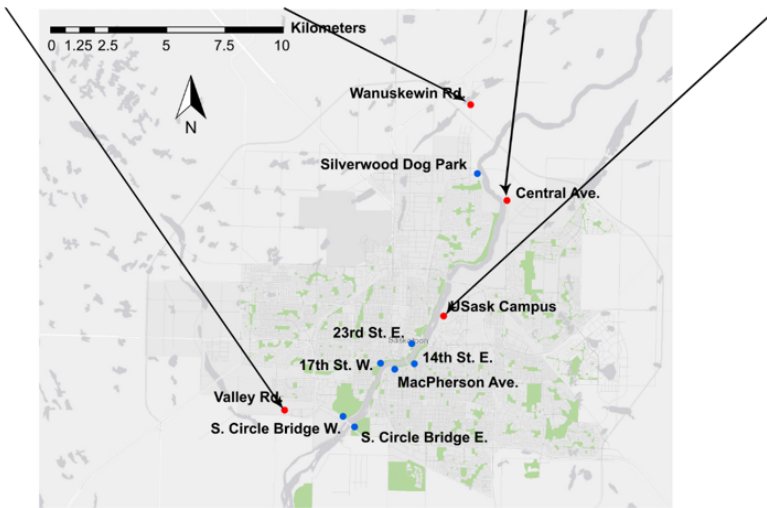
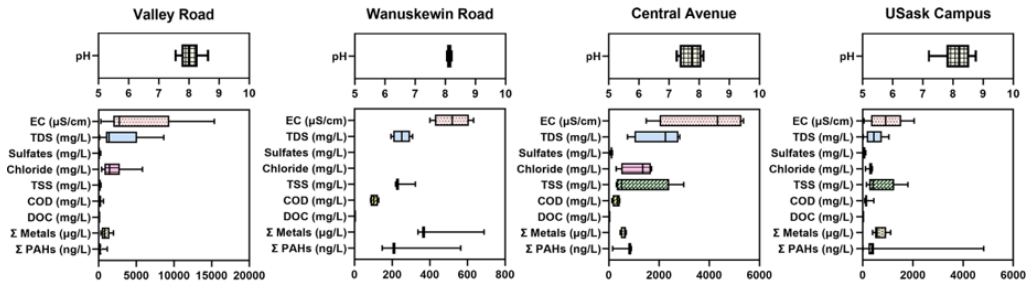


Figure 1

Map of the City of Saskatoon (CoS) indicating current snow facilities (red). Stormwater (SW) outfalls are indicated with blue dots, which are out of the scope of this study. See Table S2 for timing and distribution of sampling events. Units are contaminant-specific and error bars indicate 95% CIs.

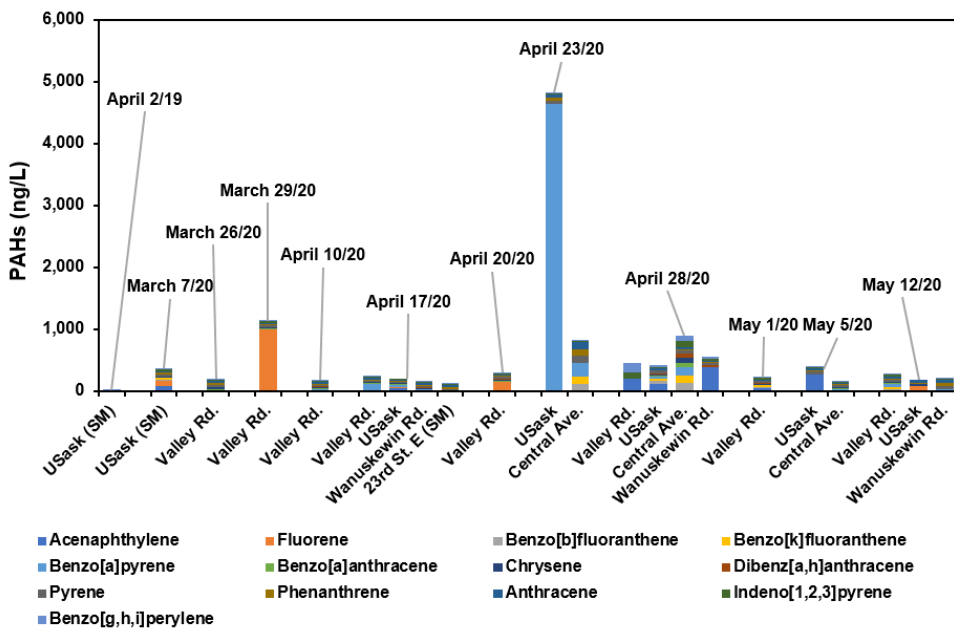
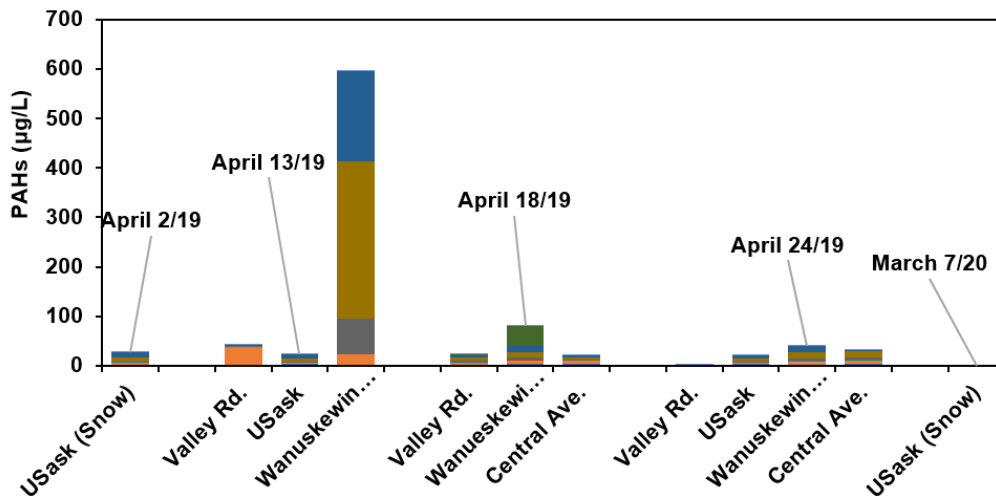


Figure 3

Sum of the analyzed suite of dissolved PAHs measured in snow piles (SPs; top) and snowmelt (SM; bottom). Note the graphs are employed on differently-scaled vertical axes.

Supplementary Files

This is a list of supplementary files associated with this preprint. Click to download.

- [PopicketalSnowmeltSIESPR.docx](#)